THE REACH OF THE CERN LARGE HADRON COLLIDER FOR GAUGE-MEDIATED SUPERSYMMETRY BREAKING MODELS

Howard Baer[1], P. G. Mercadante[1], Xerxes Tata[2] and Yili Wang[2]

[1]*Department of Physics, Florida State University, Tallahassee, FL 32306, USA*
[2]*Department of Physics and Astronomy, University of Hawaii, Honolulu, HI 96822, USA*

Abstract

We examine signals for sparticle production at the CERN Large Hadron Collider (LHC) within the framework of gauge mediated supersymmetry breaking models with a low SUSY breaking scale for four different model lines, each of which leads to qualitatively different signatures. We first examine the reach of the LHC via the canonical $\not{E}_T$ and multilepton channels that have been advocated within the mSUGRA framework. Next, we examine special features of each of these model lines that could serve to further enhance the SUSY signal over Standard Model backgrounds. We use ISAJET to evaluate the SUSY reach of experiments at the LHC. We find that the SUSY reach, measured in terms of $m_{\tilde{g}}$, is at least as large, and sometimes larger, than in the mSUGRA framework. In the best case of the co-NLSP scenario, the reach extends to $m_{\tilde{g}} \geq 3$ TeV, assuming 10 fb^{-1} of integrated luminosity.

Typeset using REVTEX

arXiv:hep-ph/0004001v1 3 Apr 2000

I. INTRODUCTION

The search for supersymmetric particles has become a standard item for on-going as well as future experiments at high energy colliders. No signal has as yet been found, and the absence of evidence has been translated to lower limits on the masses of various sparticles [1]. Since the qualitative features as well as the size of experimental signals are determined by sparticle production cross sections and decay patterns, any such interpretation can strictly speaking only be done within the framework of a particular model, most often taken to be the minimal supergravity (mSUGRA) model. While it is true that in some cases the non-observation of a signal can be translated into a sparticle mass bound in a relatively model-independent manner[1], the extraction of signals (or bounds) becomes increasingly complicated if several sparticles are expected to be simultaneously produced as, for instance, at hadron colliders such as the CERN LHC. This may be due to significant differences of sparticle mass and decay patterns from the mSUGRA expectations [2], or due to new decay modes being accessible as in gauge-mediated SUSY breaking (GMSB) models [3] with a low SUSY breaking scale, so that the gravitino is by far the lightest supersymmetric particle (LSP).

In recent years, there has been a flurry [4–8] of theoretical as well as experimental activity [9,10] on the detection of SUSY signals within the GMSB framework, where SUSY breaking is communicated from the hidden sector to the observable sector via Standard Model (SM) gauge interactions of messenger particles (which, we assume, can be classified into n_5 complete vector representations of $SU(5)$) with quantum numbers of $SU(2)$ doublets of quarks and leptons whose mass scale is characterized by M. The soft supersymmetry breaking masses for the SUSY partners of SM particles are thus proportional to the strength of their gauge interactions, so that squarks are heavier than sleptons, while the gaugino masses satisfy the usual "grand unification" mass relations, though for very different reasons. Within the minimal version of this framework, the couplings and masses of the sparticles in the observable sector are determined (at the messenger scale M) by the parameter set,

$$\Lambda, M, n_5, \tan\beta, sign(\mu), C_{grav}. \tag{1.1}$$

The parameter Λ sets the scale of sparticle masses and is the most important of these parameters. The model predictions for soft-SUSY breaking parameters at the scale M are evolved to the weak scale. The parameter $C_{grav} \geq 1$ [5] and enters only into the partial width for sparticle decays to gravitino. The decay to a gravitino is phenomenologically important only for the decay of the next to lightest supersymmetric particle (NLSP). We fix $C_{grav} = 1$ which corresponds to the fastest possible decay of the NLSP into the gravitino: for larger values of C_{grav}, the NLSP may decay with an observable decay gap (possibly improving the sensitivity to the signal), or may even pass all the way through the detector.

---

[1]For example, at LEP, it is possible to infer a bound on the mass of the right handed slepton, assuming only that it is the lightest unstable sparticle, so that it must decay via $\tilde{\ell}_R \to \ell\widetilde{Z}_1$; even here it is tacitly assumed that the decay of $\tilde{\ell}_R$ is prompt.

The phenomenological implications of the model are only weakly sensitive to M. Aside from the scale of sparticle masses, the single item that most sensitively determines sparticle signals at colliders is the identity of the NLSP. In the simplest version of model, the NLSP is either the lightest neutralino ($\widetilde{Z}_1$) with the hypercharge gaugino as its dominant component, or the lighter stau ($\tilde{\tau}_1$). In the latter case, depending on the value of $\tan\beta$, $\tilde{e}_1$ and $\tilde{\mu}_1$ may be essentially degenerate with $\tilde{\tau}_1$.

If the NLSP is a $U(1)$ gaugino-like neutralino, it dominantly decays via $\widetilde{Z}_1 \to \gamma\tilde{G}$, and SUSY events always contain two hard, isolated photons and $\not{E}_T$ (from the escaping gravitinos) in addition to jets and/or leptons. In the case where the NLSP is a stau which is significantly lighter than other sleptons, it is produced in most SUSY decay chains, and SUSY events in this scenario typically contain several tau leptons. Other light sleptons decay via $\tilde{\ell}_1 \to \ell\widetilde{Z}_1$ if the decay is allowed; otherwise as discussed in Ref. [6], these mostly decay via $\tilde{\ell}_1^- \to \tilde{\tau}_1^+ \ell^- \tau^-$ or $\tilde{\ell}_1^- \to \tilde{\tau}_1^- \ell^- \tau^+$ which (even for $C_{grav} = 1$), as long as these are not kinematically strongly suppressed, have a much larger branching ratio than for the decay $\tilde{\ell}_1 \to \ell\tilde{G}$. For the case where $m_{\tilde{\ell}_1} - m_{\tilde{\tau}_1} \leq m_\tau$ (the co-NLSP scenario), only the gravitino mode is allowed, so that we may then expect a significant multiplicity of isolated e's and μ's in SUSY events.

In a previous paper [6], we examined SUSY signals and the reach of the Fermilab Tevatron Main Injector (for integrated luminosities of 2 and 25 fb^{-1}) for representative cases for each one of these three model lines discussed in the previous paragraph. We also examined the reach for the so-called higgsino model line [2] where the NLSP is a higgsino-like neutralino. Although this does not occur in the minimal version of the GMSB framework because μ tends to be large compared to the hypercharge gaugino mass M_1, we were motivated to examine this case since experimental signals tend to be quite different because the NLSP dominantly decays via $\widetilde{Z}_1 \to h\tilde{G}$ (rather than $\widetilde{Z}_1 \to \gamma\tilde{G}$) unless this decay is suppressed by phase space. Our purpose here is to perform a similar study for the reach of the CERN Large Hadron Collider (LHC), a pp collider with a center of mass energy $\sqrt{s} = 14$ TeV, currently scheduled to begin operation in 2005. We assume throughout this paper that an integrated luminosity of 10 fb^{-1} is collected, which corresponds to a year of running at the lower value of the design luminosity.

Toward this end we examine the SUSY reach of the LHC for,

- model line A: $n_5 = 1$, $M = 1000$ TeV, $\tan\beta = 2$, $\mu > 0$, which gives a $U(1)$ gaugino-like NLSP;

- model line B: $n_5 = 2$, $M = 3\Lambda$, $\tan\beta = 15$, $\mu > 0$, for which the NLSP is a stau;

- model line C: $n_5 = 3$, $M = 3\Lambda$, $\tan\beta = 3$, $\mu > 0$, which yields the co-NLSP scenario;

- model line D: $n_5 = 2$, $M = 3\Lambda$, $\tan\beta = 3$, $\mu = -\frac{3}{4}M_1$, which gives a higgsino-like neutralino as the NLSP, which if heavy enough mainly decays via $\widetilde{Z}_1 \to h\tilde{G}$;

---

[2]These four model lines were first proposed for study at the Run II SUSY and Higgs Workshop held at Fermilab in 1998. The nomenclature used is different from that in the Workshop.

- model line E: $n_5 = 2$, $M = 3\Lambda$, $\tan\beta = 3$, $\mu = \frac{3}{4}M_1$, which also gives a higgsino-like neutralino as the NLSP, but which mainly decays via $\widetilde{Z}_1 \to Z\widetilde{G}$ as long as the decay is not suppressed by phase space.

Since we have already examined the LHC reach for model line A before [5], we will confine our attention to model lines B-E in this paper. The Tevatron reach for model lines B, C and D was studied in Ref. [6]. The reach for a gaugino-like NLSP model line, but with a slightly different set of parameters (which should have no qualitative effect on the results) was also examined in this same study. Model line E is new. The difference between D and E is that while $\widetilde{Z}_1$ mainly decays via $\widetilde{Z}_1 \to h\widetilde{Z}_1$ for model line D, the decay $\widetilde{Z}_1 \to Z\widetilde{G}$ dominates [8] in the case of model line E (assuming, of course, that these decays are kinematically unsuppressed).

For each of the model lines B-E, we first examine the reach using the strategy [11,12] for SUSY searches within the mSUGRA framework: *i.e.* the reach via the $\not{E}_T$ plus 0ℓ, $1\ell, 2\ell$ and 3ℓ inclusive channels. We expect that this (or something like it) will be the canonical strategy [15,14] for SUSY searches in the initial data samples from the LHC. For each of these model lines, we then examine whether and by how much the reach can be improved using the special features characteristic of the particular model line, *e.g.* the presence of hard, isolated photons in model line A [5].

The remainder of this paper is organized as follows. In Sec. II, we briefly discuss our simulation using the program ISAJET [13]. In Section III, we discuss the LHC reach for the four model lines B-E. We end with a summary and some concluding remarks in Sec. IV.

II. EVENT SIMULATION

We use the program ISAJET v 7.43 [13] for our simulation of SUSY events. This incorporates decay matrix elements for three body decays of gluinos, charginos and neutralinos in the event generator. The implementation of the GMSB framework into ISAJET v 7.43 has been described elsewhere [6,13] and will not be repeated here. ISAJET uses the GMSB model predictions for sparticle masses as initial conditions valid at the messenger scale M, then evolves these down to the weak scale relevant for phenomenology, and finally calculates the 'MSSM parameters' that are then used in the evaluation of sparticle cross sections and decay widths.

For detector simulation at the LHC, we use the ISAJET toy calorimeter simulation package CALSIM. We simulate calorimetry covering $-5 \leq \eta \leq 5$ with a cell size given by $\Delta\eta \times \Delta\phi = 0.05 \times 0.05$, and take the hadronic calorimeter resolution to be $50\%/\sqrt{E} \oplus 0.03$ for $|\eta| < 3$, where $\oplus$ denotes addition in quadrature, and to be $100\%/\sqrt{E} \oplus 0.07$ for $3 < |\eta| < 5$, to model the effective p_T resolution of the forward calorimeter including the effects of shower spreading, which is otherwise neglected. We take electromagnetic resolution to be $10\%/\sqrt{E} \oplus 0.01$. Although we have included these resolutions, which are typical of ATLAS [14] and CMS [15], we have made no attempt to estimate the effects of cracks, edges, and other problem regions. Much more detailed detector simulations are needed to understand the effects of such regions and of the resulting non-Gaussian tails, particularly on the $\not{E}_T$ resolution.

Jets are defined as hadronic clusters with $E_T > 25$ GeV within a cone of $\Delta R = \sqrt{\Delta\eta^2 + \Delta\phi^2} = 0.7$ with $|\eta_j| \leq 3.5$. Muons and electrons with $E_T > 10$ GeV and $|\eta_\ell| < 2.5$ are considered to be isolated if the the scalar sum of electromagnetic and hadronic E_T (not including the lepton, of course) in a cone with $\Delta R = 0.3$ about the lepton to be smaller than 5 GeV. Isolated leptons are also required to be separated from one another by $\Delta R \geq 0.3$. Photons are identified as isolated with $|\eta_\gamma| < 2.5$ and $E_T > 10$ GeV if the additional E_T within a cone of $\Delta R = 0.3$ about the photon is less than 2.5 GeV. For b-jets, we require a jet (satisfying the above jet criteria) to contain a B-hadron with $p_T \geq 15$ GeV and $|\eta_j| \leq 3$. Jets with $E_T \geq 50$ GeV are tagged [3] as a b-jet with a probability of 50%. QCD jets with $E_T = 50$ (≥ 100) GeV are misidentified as b-jet with a probability of 0.79% (2%) with a linear interpolation in between [16].

III. THE SUSY REACH OF THE LHC

In this section we identify strategies to enhance the LHC SUSY reach for GMSB models beyond what would be obtained via canonical multijet + multileptons + $\not{E}_T$ analyses [11,12,16] advocated for the mSUGRA framework. We examine the reach for model lines B-E, for which the nature of the NLSP, and hence the characteristic SUSY signals, vary with the model line. The reach of model line A has already examined previously. [5]. We use ISAJET v 7.43 to compute signal cross sections, after incorporating acceptances to simulate the experimental conditions at the LHC together with additional cuts that serve to separate the SUSY signal from SM backgrounds.

A. Model Line B: The Stau NLSP model line

To realize the case of the stau NLSP, we take $n_5 = 2$, $M = 3\Lambda$, $\mu > 0$, and choose $\tan\beta = 15$ to ensure that the stau is light enough for other sleptons to be able to decay to it. It is worth noting that although $m_{\tilde\tau_1} < m_{\tilde\ell_1}$, the sleptons are all sufficiently close in mass so that generally speaking the phase space for chargino and neutralino decays to staus and other sleptons is not very different. For $\Lambda \gtrsim 30$ TeV, $m_{\tilde\tau_1} \lesssim m_{\widetilde Z_1}$, but for $\Lambda \lesssim 31$ TeV, $\widetilde Z_1 \to \tau\tilde\tau_1$ is kinematically forbidden, and $\widetilde Z_1$ would decay via the four body decay $\widetilde Z_1 \to \nu_\tau\tilde\tau_1 W^*$ (which is not yet included in ISAJET) or via $\widetilde Z_1 \to \gamma\tilde G$. In our study, we consider $\Lambda \geq 35$ TeV, the range safe from LEP constraints.

In Fig. 1, we show cross sections for various sparticle production processes at the LHC. For $\Lambda \leq 125$ TeV ($m_{\tilde g} \lesssim 1.8$ TeV), squark and gluino production (solid line) dominates, while for larger values of Λ electroweak production of various charginos and neutralinos (dashed line) are the dominant SUSY process. For cross sections in the range of interest at the LHC, direct slepton and sneutrino production occurs at $\sim \frac{1}{3}$ the rate for chargino and neutralino production. Cascade decays of squarks and gluinos naturally lead to events with n leptons + m jets + $\not{E}_T$. These event topologies may also arise from the production of

---

[3]For the purposes of reconstructing h produced via $\widetilde Z_1 \to h\tilde G$ for model line D, we assume that softer b-jets can also be tagged, but with a reduced efficiency as detailed in Sec. III C.

gluinos and squarks in association with a chargino or a neutralino, and also from chargino and neutralino production.

The decay patterns of charginos, neutralinos and sleptons have been discussed in detail in Ref. [6] and we will only summarize the results here. The two body decay $\widetilde{W}_1 \to \tilde{\tau}_1 \nu$ is always accessible, and dominates for $\Lambda \leq 45$ TeV ($m_{\widetilde{W}_1} \lesssim 210$ GeV). The decay rate for $\widetilde{W}_1 \to W\widetilde{Z}_1$ becomes comparable to that for $\widetilde{W}_1 \to \tilde{\tau}_1 \nu$ for $\Lambda \sim 60$ TeV, while for very heavy charginos ($m_{\widetilde{W}_1} \gtrsim 900$ GeV), the branching ratio for $\widetilde{W}_1 \to W\widetilde{Z}_1$ is around 75%. Turning to neutralinos, $\widetilde{Z}_2 \to \tilde{\tau}_1 \tau$ is the main decay mode of $\widetilde{Z}_2$ if $m_{\widetilde{Z}_2} \lesssim 300$ GeV. The decay $\widetilde{Z}_2 \to \widetilde{Z}_1 h$ is only important for $\Lambda \gtrsim 55$ TeV ($m_{\widetilde{Z}_2} \gtrsim 270$ GeV) and becomes dominant for $\Lambda \gtrsim 80$ TeV ($m_{\widetilde{Z}_2} \gtrsim 400$ GeV). Branching fractions for $\widetilde{Z}_2 \to \tilde{\ell}_1 \ell$ ($\ell = e, \mu$) may also be significant and vary from 20% each for $\Lambda = 35$ TeV to $< 1\%$ for $\Lambda = 180$ TeV. The branching fraction for the decay $\widetilde{Z}_2 \to Z\widetilde{Z}_1$ is $\sim 5\%$ if this decay is kinematically accessible. For small enough Λ, the lightest neutralino $\widetilde{Z}_1$ mainly decays via $\widetilde{Z}_1 \to \tilde{\tau}_1 \tau$, but for large enough values of Λ its decay to other sleptons are also important, and together exceed the decays to stau when for $\Lambda > 80$ TeV ($m_{\widetilde{Z}_1} \lesssim 220$ GeV). Finally, for small values of Λ accessible at Tevatron upgrades, $\tilde{\ell}_1$ can only decay via $\tilde{\ell}_1 \to \ell \widetilde{Z}_1$. For larger Λ, this channel is closed, the neutralino is virtual and then the decays $\tilde{\ell}_1^- \to \tilde{\tau}_1^+ \ell^- \tau^-$ and $\tilde{\ell}_1^- \to \tilde{\tau}_1^- \ell^- \tau^+$ dominate. However, the decay $\tilde{\ell}_1 \to \ell \widetilde{G}$ also becomes significant (branching fraction $\geq$10% for $\Lambda \gtrsim 120$ TeV) if Λ is large enough.

We begin our discussion of the LHC reach via canonical searches in the multijet plus multilepton plus $\slashed{E}_T$ channels as discussed in Ref. [11,12]. For squark and gluino production, the p_T of the primary jets from gluinos (squarks decay to gluinos), as well as the $\slashed{E}_T$, are expected to scale with $m_{\tilde{g}}$. Since the signal decreases with increasing $m_{\tilde{g}}$, its separation from SM backgrounds can be optimized by requiring cuts on jets and $\slashed{E}_T$ that scale with the gluino mass. The momenta of leptons, produced far down in the cascade decay chain from chargino and neutralino daughters, do not scale in energy the same way as $\slashed{E}_T$ or energies of jets which are produced in the first step of the decay cascade. Following Ref. [11,12], we introduce the running cut variable E_T^c, and require that the signal events satisfy:

- $n_{jet} \geq 2$ (with $E_{T(j)} > 100$ GeV);

- the transverse sphericity, $S_T \geq 0.2$;

- $E_T(j_1)$, $E_T(j_2) > E_T^c$ and $\slashed{E}_T > E_T^c$;

- for 1ℓ signal, $p_T(\ell) > 20$ GeV and $M_T(\ell, \slashed{E}_T) > 100$ GeV;

- for $n \geq 2$ lepton signal, $p_T(\ell_1, \ell_2) > 20$ GeV,

in addition to the basic acceptance cuts. We classify signal events according to their lepton topology into the nonleptonic $\slashed{E}_T$ + jets channel, the opposite-sign (OS) dilepton + jets $+\slashed{E}_T$ channel, the same-sign (SS) dilepton + jets $+\slashed{E}_T$ channel, and the multilepton + jets $+\slashed{E}_T$ channel with $n_\ell \geq 3$. Throughout this paper, we consider a signal to be observable in a particular channel if there are at least 5 signal events and also the signal has a statistical significance ≥ 5, assuming 10 fb^{-1} of integrated luminosity. We study the observability by varying E_T^c between 100 and 500 GeV in steps of 100 GeV.

6

The dominant SM backgrounds are W, γ^* or Z + jet production, $t\bar{t}$ production and vector boson pair production. Since our analysis cuts are identical to those in Ref. [11,12], we do not re-compute these backgrounds but instead use the background cross sections as a function of E_T^c given in these papers in our analysis. [4]

The results of our computation of the reach of the LHC using the mSUGRA cuts are summarized in Fig 2 where we show the maximum $\sigma_S/\sqrt{\sigma_B}$ as a function of E_T^c, requiring further that there be at least 5 signal events per 10 fb^{-1}. For each value of Λ that we studied, the number on the various lines denotes the E_T^c value for which the signal is observable according to our criteria, and for which the signal significance is the greatest (subject to the five event minimum), i.e. a 2 denotes $E_T^c = 200$ GeV yields the best significance, *etc.* In other words, this number provides information about the optimal strategy for the particular value of Λ. The different lines correspond to the different event topologies: $0\ell+\not{E}_T$ (lower solid), $1\ell+\not{E}_T$ (upper solid), SS dileptons $+\not{E}_T$ (dashed), OS dileptons $+\not{E}_T$ (dotted) and trileptons (dot-dashed). The horizontal line denotes the 5σ level for an integrated luminosity of 10 fb^{-1}.

We see from the figure that unlike the case of the mSUGRA framework, the inclusive 3ℓ channel provides the greatest reach. This is presumably because of additional leptons that come from slepton decays to the gravitino, or as secondaries of daughter taus produced via the decay of the stau NLSP. The $\not{E}_T$ signal (with a lepton veto) gives a rather poor reach for essentially the same reason. We can probe Λ values beyond 150 GeV which corresponds to a gluino in excess of 2 TeV in this channel. Notice also that if $\Lambda \leq 125$ TeV ($m_{\tilde{g}} \lesssim 1.8$ TeV) confirmatory signals should appear in several other channels. For comparison, we note that even for an integrated luminosity of 25 fb^{-1}, the reach of the Tevatron was projected [6] to be about 50 TeV.

Next, we examine whether we can extend the reach by requiring the presence of additional tagged τ leptons. In Table I, we show the signal cross section for $\Lambda = 120$ and 160 TeV, with events classified first by the number of identified taus, and then by the lepton multiplicity. Here, a jet with $E_T \geq 40$ GeV is identified as a tau if it has one or three charged prongs with $p_T \geq 2$ GeV in a $10°$ cone about the jet axis, with no other tracks in the corresponding $30°$ cone. If the number of charged prongs is three, we require their net charge to be ± 1 and the invariant mass to be smaller than m_τ. QCD fakes are included with the same algorithm used in Ref. [6]. The cross sections shown in Table I are obtained with just $\not{E}_T \geq 50$ GeV in addition to the basic lepton and τ identification cuts. We see that even with this minimal requirement, the cross section for $n_e + n_\mu + n_\tau \geq 4$ events is just 3.25 (.92) fb for $\Lambda = 120(160)$ TeV. Since these channels all suffer from physics, and more importantly instrumental, backgrounds from SM sources, we conclude that tagging hadronically decaying taus is unlikely to improve the reach for this model line: cuts to remove these will reduce the signal to below the observable level for Λ values where the canonical strategy does not lead to a detectable signal.

We also attempted to extract the signal via "clean" multilepton plus multi-tau channels where we veto events with jets that are not identified as taus. We found that typically the

---

[4]We caution the reader that these backgrounds were computed using CTEQ2L structure functions, while for the signal CTEQ3L [17] structure functions have been used.

signal reduces by an order of magnitude (or more, depending on the transverse momentum threshold for the jet veto) and falls well below the one event level in all the channels. We thus conclude that the canonical SUSY search strategy [12] via multilepton channels provides the largest reach for model line B.

B. Model Line C: The co-NLSP Model Line.

For this model line, $\tilde{e}_1$, $\tilde{\mu}_1$ and $\tilde{\tau}_1$ are approximately degenerate, and $\tilde{e}_1$ and $\tilde{\mu}_1$ cannot decay to $\tilde{\tau}_1$. To realize this, we choose $n_5 = 3$ and $\tan\beta = 3$ with other parameters as before. Various sparticle production cross sections are shown in Fig. 3. We see that while production of squarks and gluinos dominates for $\Lambda \leq 125$ TeV ($m_{\tilde{q}} \leq 2.3$ TeV, $m_{\tilde{g}} \leq 2.5$ TeV), slepton pair production is dominant for $\Lambda \gtrsim 125$ TeV (corresponding to $m_{\tilde{l}} \gtrsim 380$ GeV).

In this model line, gluinos decay directly to squarks. The left-squarks typically cascade to $\widetilde{W}_1$ and $\widetilde{Z}_2$ which then decay to the lightest neutralino, while $\tilde{q}_R$ mostly decays directly to $\widetilde{Z}_1$. The sparticle decay patterns have been discussed in Ref. [6]. The lightest neutralino decays via $\widetilde{Z}_1 \to \tilde{\ell}_1 \ell$, ($\ell = e$, μ, and τ), with branching fractions essentially independent of the lepton flavour. Sleptons and sneutrinos decay via $\tilde{f}_2 \to f\widetilde{Z}_1$ while $\tilde{f}_1 \to f\tilde{G}$ ($f = \ell, \nu$). For very small Λ (excluded by LEP 2 since the slepton is then very light), the charginos can only decay via $\widetilde{W}_1 \to \tilde{\tau}_1 \nu_\tau$ [5] but over much of the allowed range of Λ the decays $\widetilde{W}_1 \to \tilde{\nu}\ell, \nu\tilde{\ell}$ dominate and have (approximately) flavour-independent branching fractions. The decay $\widetilde{W}_1 \to W\widetilde{Z}_1$ also becomes significant for charginos heavier than $\gtrsim 200$ GeV, and has a branching fraction that decreases from a maximum of $\sim 30\%$ to $\sim 15\%$ as Λ increases to 130 TeV. The second lightest neutralino $\widetilde{Z}_2$ decays to sleptons with branching fractions more or less independent of the lepton flavour. Decays to the heavier (mainly left-handed) sleptons and sneutrinos dominate when these are not kinematically suppressed. The branching fraction for the decay $\widetilde{Z}_2 \to \widetilde{Z}_1 h$ is also significant once this decay is allowed, and the branching fraction reduces from a maximum of 25% to below 15% for $\Lambda = 130$ TeV. Neutralino decays to Z are negligible. An inspection of these decay patterns shows that it would be natural to expect events with a large multiplicity of isolated leptons(e and μ) from sparticle production, so that multilepton plus $\not{E}_T$ events should provide the best reach.

The naturally high lepton multiplicity in these events led us to focus on the essentially background-free $n_\ell \geq 4$ lepton plus $\not{E}_T$ channel. We have not attempted to make a quantitative calculation of the background but have instead contented ourselves with trying to bound cross sections for physics sources of such events. These include,

- $4t$ production with $\sigma(4t) = 6$ fb [18], which yields $\sigma(4\ell) = 0.014$ fb (neglecting isolated leptons [6] from b decays);

---

[5]This decay proceeds mainly via the higgsino component; as a result, decays to other slepton flavours are strongly suppressed.

[6]The cross section for 3 leptons from the decays of Ws is 0.25 fb; since the branching fraction for leptonic b decays is about 0.22, we conclude that as long as the lepton from b is isolated less than $\sim 1/20$ of the time, this background is smaller than the 4ℓ level estimated above.

- $4W$ production with $\sigma(4W) = 1\ fb$ [19], which yields $\sigma(4\ell) = 2.3 \times 10^{-3}\ fb$;

- WWZ production with $\sigma(WWZ) = 150\ fb$ [20], which yields $\sigma(4\ell) = 2.4 \times 10^{-2}\ fb$ (here we assume that events $Z \to \ell\bar{\ell}$ can be removed by a mass cut, and retain leptons only from $Z \to \tau\bar{\tau}, \tau \to \ell\nu\bar{\nu}$);

- ZZ production with $\sigma(ZZ) = 10$ pb, which yields $\sigma(4\ell) = 0.11\ fb$ where, once again, we assume that the leptons come only via $Z \to \tau\bar{\tau}$ decays. These events tend not to have a large $\not{E}_T$ and softer leptons, and the background can be greatly reduced by a cut on $\not{E}_T$ and the lepton p_T.

Turning to the signal, we show the distributions of the two hardest leptons in $\geq 4\ell$ SUSY events in Fig. 4 for four choices of Λ. We see that requiring these leptons to be harder than 50 GeV reduces the signal by just a few percent for $\Lambda = 120$ TeV. Even for $\Lambda = 35$ TeV, the reduction is just 40%, which is very affordable because of enormous SUSY cross sections at the LHC. Although we do not show this, we have also checked that the signal loss from requiring $\not{E}_T \geq 100$ GeV is again only a few percent for $\Lambda = 120$ TeV.

To obtain the LHC reach via the $\geq 4\ell$ signal for model line C, we thus require:

- $\not{E}_T > 100$ GeV;

- $p_T(\ell_1), p_T(\ell_2) > 50$ GeV;

- a Z veto – we remove events where with $\ell^+\ell^-$ pairs that reconstruct the Z mass to within 10 GeV.

We assume that these cuts reduce the SM physics backgrounds already found to be below $0.2\ fb$ to completely negligible levels. Assuming that instrumental backgrounds are under control, we then estimate the reach for this model line by requiring at least five signal events in 10 fb^{-1} as illustrated in Fig. 5 where we show the signal cross section with $n_\ell \geq 4$ versus Λ. We see that the reach extends up to $\Lambda = 155$ TeV, which corresponds to squarks (gluinos) just below (above) 3 TeV, to be compared with the reach of $\Lambda \sim 55$ TeV [6] for an integrated luminosity of 25 fb^{-1} at the Tevatron.

Since the sleptons are the co-NLSPs in this scenario, we have also examined the range of parameters where these can be directly observed at the LHC. We follow the general strategy for slepton searches at the LHC detailed in Ref. [21], with some modifications to optimize for the GMSB scenario. The analysis cuts that we impose are,

- exactly two isolated same flavor OS leptons, each with $p_T(l) \geq 20$ GeV;

- $\not{E}_T > 100$ GeV;

- number of jets with $E_{Tj} \geq 25$ GeV is zero (jet veto);

- $\Delta\phi(p_{T(\ell\bar{\ell}')}, \not{E}_T) \geq 160°$.

These cuts above are exactly the same as in Ref. [21]. For the final cut, however, we choose instead,

- $p_T(\ell_1) > 80$ GeV, $p_T(\ell_2) > 60$ GeV and $\Delta\phi(\ell_1, \ell_2) < 140°$.

9

The major SM background at the LHC come from $t\bar{t}$ production and WW production. The jet veto is crucial to reduce the top quark background. In our simulation, we have assumed that jets can be vetoed with an efficiency of 99%. After these cuts, the $t\bar{t}$ background is 0.06 fb, while the WW background is 0.038 fb, so that the total SM background $\sim 0.1\ fb$ and the minimum detectable cross section corresponds to 5 events per 10 fb^{-1}.

The signal cross section for opposite sign dilepton from just slepton production (slepton, chargino and neutralino production) is shown by the dashed (solid) line in Fig. 6. We see that except for the $\Lambda = 30$ TeV case (corresponding to $m_{\tilde{\ell}_1} = 99$ GeV, just beyond the current bound from LEP 2) the signal dominantly comes from slepton pair production because $m_{\widetilde{W}_1} \sim m_{\widetilde{Z}_2} \gg m_{\tilde{\ell}}$. The reason the dashed curve falls for low values of Λ is the inefficiency of our cuts (which have been optimized for heavier sleptons) for such light sleptons. Nonetheless, even with these cuts [7] there is ample signal for SUSY not to evade detection at the LHC. We see that the reach extends up to $\Lambda = 90$ TeV corresponding to $m_{\tilde{\ell}_1} \simeq 280$ GeV. The reason that the reach in slepton mass is significantly smaller than the corresponding reach within the mSUGRA framework is because the production of $\tilde{\ell}_L$ and $\tilde{\nu}_L$, which was the main contributor to the slepton cross section in mSUGRA, is now kinematically suppressed: *i.e.* within the GMSB, $\tilde{\ell}_R\tilde{\ell}_R$ production forms the bulk of the slepton cross section.

C. Model Line D: A Higgsino NLSP with $\widetilde{Z}_1 \to h\tilde{G}$

Within the minimal GMSB framework, the lightest neutralino is dominantly the hypercharge gaugino. However, since the phenomenology is very sensitive to the nature of the NLSP, we entertain the possibility that in other models, the NLSP may be higgsino-like. We do not attempt to construct any model, but take a purely phenomenological approach, by letting μ to be a free parameter instead of fixing it via radiative electroweak symmetry breaking conditions. [8] If μ is smaller than the hypercharge gaugino mass M_1, the NLSP will indeed contain a large higgsino component. We take $n_5 = 2$, $\tan\beta = 3$, $M/\Lambda = 3$, $C_{grav} = 1$ but fix $\mu = -\frac{3}{4}M_1$ rather than the value obtained from radiative electroweak symmetry breaking. Within this 'small μ' model line, the two lightest neutralinos and the lighter chargino are Higgsino-like and close in mass, while the heavier charginos and neutralinos are gaugino-like. The $\widetilde{Z}_1$ is the NLSP and the $\widetilde{Z}_2$ and $\widetilde{W}_1$ are only little heavier. The fermions from $\widetilde{W}_1$ and $\widetilde{Z}_2$ decays to $\widetilde{Z}_1$ will be rather soft. For this sign of μ, the NLSP dominantly decays via $\widetilde{Z}_1 \to h\tilde{G}$ if the $\widetilde{Z}_1$ is heavy enough ($\Lambda \gtrsim 80$ TeV) so that the decay is not suppressed by phase space. The mass m_h of the lighter Higgs boson is just above 100 GeV, independent of Λ.

If $\Lambda \gtrsim 50$ TeV (smaller values of Λ would have charginos and neutralinos accessible at

---

[7]Other cuts detailed in Ref. [21] would be better suited for detection of these lighter sleptons, and also for separating the slepton signal from the signal from charginos.

[8]For instance, additional interactions needed to generate μ and also the B-parameter in this framework could conceivably alter the relation between μ and the gaugino masses.

LEP 2), we see from Fig. 7 that the production of charginos and neutralinos is the dominant source of sparticles at the LHC. Gluinos and squarks are relatively heavy so that their production becomes rapidly suppressed as Λ is increased. Slepton and sneutrino production forms only a percent of the total SUSY cross section. As already noted, the branching fraction for the two body decay $\widetilde{Z}_1 \to \tilde{G}h$ exceeds 50% if $\Lambda \gtrsim 80$ TeV, and becomes $\sim 75\%$ for $\Lambda \gtrsim 200$ TeV [6]. The decays $\widetilde{Z}_1 \to Z\tilde{G}$ account for essentially all the remaining decays of $\widetilde{Z}_1$ since $\widetilde{Z}_1 \to \gamma\tilde{G}$ with a branching fraction of at most a few if $\Lambda \geq 120$ TeV. The heavier neutralino $\widetilde{Z}_2$ as well as the lighter chargino $\widetilde{W}_1$ decay via three body decays, but their decay products are soft since they are only a little heavier than $\widetilde{Z}_1$. As a result, signatures for $\widetilde{W}_1\widetilde{W}_1$ or $\widetilde{Z}_i\widetilde{W}_1$ production closely resemble those for $\widetilde{Z}_1\widetilde{Z}_1$ production.

We first consider the reach via the canonical missing E_T [11] and multilepton analyses [12]. The results of our computation are shown in Fig. 8. This figure corresponds to Fig. 2 for model line B and, in fact, is qualitatively quite similar to it. Despite the fact that the $\widetilde{Z}_1$ decays mainly to the light Higgs boson for $\Lambda \geq 120$ TeV, the best reach, which is obtained in the $n_\ell \geq 3$ leptons channel, extends out to $\Lambda = 140$ TeV corresponding to $m_{\tilde{g}} = 2$ TeV, with squarks only slightly heavier. The reach in 1 lepton and 2 OS leptons channels are comparable, up to $\Lambda = 130$ TeV, while the zero lepton channel again gives the poorest reach. To understand this, we first note that although for these large values of Λ chargino and neutralino production dominates the total cross section, gluino and squark production events (which can be detected much more efficiently) form a significant portion of the cross section after the selection cuts: events from the lighter chargino and $\widetilde{Z}_{1,2}$ production (these have masses of just ~ 300 GeV) pass the hard selection cuts with very low efficiency since $m_{\widetilde{W}_1} \sim m_{\widetilde{Z}_1} \sim m_{\widetilde{Z}_2} \sim 300$ GeV. Gluinos decay to $t\bar{t}\widetilde{Z}_{1,2}$ or $tb\widetilde{W}_1$ with a branching fraction of 60%, with the bulk of the remaining decays into the heavier chargino and to the heaviest neutralino. Squarks mainly decay to the gaugino-like $\widetilde{W}_2$, $\widetilde{Z}_3$ and $\widetilde{Z}_4$ ($\tilde{q}_R$ mainly decays to $\widetilde{Z}_3$); $\widetilde{W}_2$ and $\widetilde{Z}_4$ mainly decay via two body decays to vector bosons or the lightest Higgs scalar h and a lighter chargino or neutralino, and at a few percent into left sleptons and sneutrinos. The $\widetilde{Z}_3$, on the other hand, mostly decays via $\widetilde{Z}_3 \to \tilde{\ell}_R\ell$. For $\Lambda = 140$ GeV, $\tilde{\ell}_L$ and $\tilde{\nu}$ mainly cascade decay to $\widetilde{Z}_3$ which then mostly decays into right sleptons. Notice that if $\tilde{\ell}_L$, $\tilde{\nu}$ or $\widetilde{Z}_3$ are produced at any step, their decays are by themselves likely to give two hard leptons, resulting in multiple leptons from squark and gluino events. For the higgsino NLSP case, the cascade decay chains are more complicated than in the canonical mSUGRA case, because of the dominance of gluino and squark decays to the heavier charginos and neutralinos, and in the gluino case, also to top quarks.

For values of Λ close to the LHC reach in Fig. 8, the NLSP dominantly decays via $\widetilde{Z}_1 \to \tilde{G}h$. In this case, since h mainly decays via $h \to b\bar{b}$, the SUSY signal will contain b-jets in addition to leptons, $\not{E}_T$ and possibly photons (if one of the NLSPs decays via the photon mode which has a branching fraction of a few percent [6]). We were, therefore, led to examine whether requiring tagged b-jets in SUSY events can increase the reach via the observation of lighter chargino and neutralino events which have a production cross section ≥ 300 fb. The dominant SM background to multi-b plus large $\not{E}_T$ events presumably comes from $t\bar{t}$ production. We examined several event topologies as well as distributions from the signal and from the top background and concluded that the most promising channel was the one with just two tagged b-jets channel, with the following cuts to reduce the top background:

1. $\not{E}_T \geq 100$ GeV;

2. $p_T(b-jet) > 50$ GeV;

3. $\not{E}_T + \Sigma E_{Tj} \geq 1500$ GeV, where the sum extends over untagged jets.

The results of our computation are shown in Table II. We show the signal cross sections for $\Lambda = 140, 150$ and 160 TeV and compare these with the top background for two choices for the b mistagging probability. The set of columns labelled 2% assume the b mis-tagging probability introduced in Sec. II. The columns labelled 1% assume the mis-tagging probability to be half this. The statistical significance $\frac{N_S}{\sqrt{N_B}}$ is for 10 fb^{-1}. We see from the Table that for the canonical mis-tag rate even the $\Lambda = 150$ TeV case falls just short of observability but appears to pass our observability criteria with the more optimistic assumptions about b-mistagging. In view of the fact that $t\bar{t}$ is the only background we have included in our computation, and further, that the reach is only marginally increased above this background, we conclude that the canonical multilepton search is sufficient to probe model line D at the LHC, and further that the LHC reach extends out to $\Lambda = 140 - 145$ TeV (corresponding to $m_{\tilde{g}} = 2$ TeV, with squarks a little heavier).

We have also examined the ≥ 3 tagged b-jet channel which without the hardness cut 3 has a much better S/B ratio. The signal cross section, in this channel, is small and it is difficult to make other cuts (to reduce the top background) without reducing the signal to below the level of observability. It is conceivable though that with an integrated luminosity of 100 fb^{-1} this channel may prove more promising; the background from $4b$ production would then have to be carefully examined.

Finally, we examine whether it is possible to identify the Higgs boson, which is the characteristic feature of model line D, in SUSY events. It has been known for many years that the presence of Higgs bosons can be inferred either via the multiplicity of b-jets in SUSY events [22], or more directly, via the reconstruction of a mass bump in the M_{bb} distribution [11,23]. We follow the latter approach, and attempt to reconstruct the lighter Higgs boson (which has a mass of about 104 GeV) in SUSY events in channels with identified b-jets for $\Lambda = 80$ TeV and $\Lambda = 110$ TeV. Again top quark pair production is the major SM background. To reduce this, we require that

$$\not{E}_T + \Sigma E_T(jets) \geq E_0,$$

where the sum extends over untagged b-jets with $E_T \geq 100$ GeV. We adjust the cut variable E_0 depending on Λ and on the event topology. In particular, we choose $E_0 = 1300$ (900) GeV for two (three) tagged b events if $\Lambda = 80$ TeV, and 1500 (1100) GeV if $\Lambda = 110$ TeV. We found that we were unable to obtain a mass bump (with these as well as several other selection cuts that we examined) even though the cross section was quite large. We traced this to the fact that most of the time one of the two b-jets from h decay usually has $p_T \leq 50$ GeV, and so fails our tagging criteria. In other words, the two b-jets from the decay of h are almost never simultaneously tagged. To enable the identification of h in SUSY events, we include in our analysis that b-jets with E_T between 25 and 50 GeV may also be tagged, but with a reduced efficiency which we take to be [16] $0.015 \times p_T - 0.25$. We extrapolate our previous mistagging rate down to 25 GeV.

12

The M_{bb} distribution in the two and three tagged b channels after the cuts above is shown in Fig. 9 for $\Lambda = 80$ and 110 TeV. The dashed histograms are the $t\bar{t}$ background while the solid histograms are the sum of the signal and background. We see that there is a clear peak close to m_h in the M_{bb} distributions in the two tagged b channel. The distribution cuts off at the low end because each tagged jet has at least 25 GeV, while the continuum beyond the peak corresponds to combinations where one or both b-jets come from sources other than Higgs decay or are QCD jets that have been mistagged. The corresponding peaks for the three b channel, though present, is not as distinctive, presumably because the combinatorial background also contributes to the continuum.

We also examined the distribution of p_T of the Higgs boson reconstructed from two tagged bs with $M_{bb} \simeq m_h$; *i.e.* in the peak. We might expect that this distribution would scale with $m_{\widetilde{Z}_1}$, and hence provide a measure of Λ. We found, however, that the distributions for Λ in the 80-110 TeV range overlapped quite substantially, and conclude that it is difficult to measure Λ this way. We attribute this to the fact that the change in $m_{\widetilde{Z}_1}$ is rather limited (160-220 GeV), and further, that h can also be produced at an earlier stage in the cascade, thereby smearing this distribution. For larger values of Λ the event rate appears to be too low for this to be feasible.

D. Model Line E: Higgsino NLSP with $\widetilde{Z}_1 \to Z\tilde{G}$

If the NLSP contains a significant fraction of the SUSY partner of the would-be neutral Goldstone boson (that becomes the longitudinal component of the Z by the Higgs mechanism), it would preferentially decay via $\widetilde{Z}_1 \to Z\tilde{G}$ provided that this decay is not kinematically suppressed. It has recently been pointed out that this situation is indeed realized [8] for a Higgsino model line where the sign of μ is flipped relative to that in model line D above. We thus consider a final model line with $n_5 = 2$, $\tan\beta = 3$, $M/\Lambda = 3$, $C_{grav} = 1$ but fix $\mu = \frac{3}{4}M_1$. The decay pattern of the neutralino NLSP is shown in Fig. 10. We see that for $\Lambda \geq 85$ TeV (corresponding to an NLSP heavier than 140 GeV) the decay $\widetilde{Z}_1 \to Z\tilde{G}$ dominates, while for smaller masses, the photon decay is the main mode. [9] The branching fraction for the decay $\widetilde{Z}_1 \to h\tilde{G}$ becomes significant only when Λ is rather large.

The main sparticle production cross sections are shown in Fig. 11 which is qualitatively very similar to Fig. 7. This should not be surprising because changing the sign of μ qualitatively affects only the NLSP decay pattern, though of course there is some effect on the chargino and neutralino masses and mixing angles. Again, as in model line D, the mass gap between $\widetilde{W}_1$ or $\widetilde{Z}_2$ and $\widetilde{Z}_1$ is not large, so that $\widetilde{W}_1$ and $\widetilde{Z}_2$ decays are similar to those from the decay of just the NLSP because the remaining decay products tend to be soft.

The reach of the LHC via the canonical $\not{E}_T$ and multilepton channels is illustrated in Fig. 12. As before, the number on the curves denotes the E_T^c value that optimizes the signal. Again, the upper (lower) solid curve denotes the trilepton (zero lepton) plus $\not{E}_T$ channel. The main difference from Fig. 8 is that the greatest reach, which again extends

---

[9]In this case the search strategy would be similar to that for model line A, or via the inclusive $Z\gamma$ search discussed at the end of this section.

out to 140 TeV (corresponding to $m_{\tilde{g}} = 2$ TeV, with squarks marginally heavier), is now obtained via the single lepton channel. It may seem surprising that the reach via multilepton signals degrades relative to model line D where NLSP decays are not expected to lead to isolated leptons. To understand this, we examined the decay patterns of sparticles (for $\Lambda = 140$ TeV), and found that, except for $\widetilde{Z}_1$, these are very similar for these two model lines. The big difference is that the branching fraction for $\widetilde{Z}_3 \to \tilde{\ell}_R \ell$ which was 26% per lepton flavour for model line D is now about 19%, while there is a corresponding increase in $\widetilde{Z}_3 \to \widetilde{W}_1 W$ decay. Since the presence of $\widetilde{Z}_3$ in a cascade decay chain frequently results in two leptons (see the corresponding discussion for model line D), it is not surprising that the inclusive trilepton signal is reduced relative to model line D. Indeed we have checked that for $E_T^c \geq 200$ GeV, this signal, although it has a large statistical significance, falls below the five event level (for $\Lambda \geq 140$ TeV), so that we are forced to lower E_T^c to 100 GeV for which the SM background [12] is much larger. [10]

We now examine whether the LHC reach can be extended by using the feature that NLSP mostly decays via $\widetilde{Z}_1 \to \tilde{G}Z$, so that a significant fraction of SUSY events would contain a real Z boson in addition to jets, leptons and $\not{E}_T$ [24]. Since the Z can be identified via its leptonic decay, we focus on events with an identified Z together with either two jets with $E_{Tj} \geq 50$ GeV or additional leptons. To further suppress backgrounds, we found it was necessary to require a large $\not{E}_T$ in these events. The signal cross sections for three values of Λ just beyond the reach in Fig. 12, together with the main sources of SM backgrounds, are shown in Table III for $\not{E}_T \geq 230$ GeV. Here $\ell^+\ell^-$ pairs with $|M(\ell^+\ell^-) - M_Z| \leq 10$ GeV are identified as a Z. We see from this Table that the dominant background comes from $t\bar{t}$ production where the leptons from top decay accidentally reconstruct the Z mass. We also see that with these cuts the signal falls below the observable level, though it should be noted that all these cases would be observable for an integrated luminosity $\sim 35 - 40 \ fb^{-1}$. Two comments are worth noting.

- The signal cross section for two identified Z bosons falls below the observable level. This can even be seen from Fig. 11 and Fig. 10 where the total SUSY production cross section ($\sim 330 \ fb$) and branching ratio (75%) for $\widetilde{Z}_1 \to Z\tilde{G}$ for $\Lambda = 150$ TeV yields in $330 \times (0.75)^2 \times (0.06)^2 \times 10 \simeq 7$ events even before any acceptance cuts.

- The dominant background from tops in Table III mainly contributes to the Z plus two jet channel, and is completely negligible for Z plus lepton channels. We have checked though that the Z plus two jet channel accounts for about 70-80% of the signal, so that the total signal in just the Z plus lepton channels again falls below the observable level.

Motivated by the fact that the branching fraction for $\widetilde{Z}_1 \to \gamma\tilde{G}$ is $\sim$10% for $\Lambda \sim 140$ TeV, we have also examined whether inclusive $Z\gamma$ signals could extend the LHC reach. Toward this end we computed SM backgrounds from Zj, $WZ + ZZ$ and $t\bar{t}$ production, where a photon from radiation or the decay of a hadron is accidently isolated, using ISAJET. We also estimated the background from $Z\gamma$ production (this process is not included in ISAJET)

---

[10]We mention that with 20 fb^{-1} the trilepton channel would again yield the best reach.

by introducing the $2 \rightarrow 2 \ q\bar{q} \rightarrow Z\gamma$ process into a private version of ISAJET, and ignoring spin correlations for leptons from Z decay. We search for events in the inclusive $Z\gamma$ channel where the Z is identified by its leptonic decay and the isolated photon has $E_{T\gamma} \geq 25$ GeV. We also require $\not{E}_T \geq 100$ GeV. This last cut completely eliminates the physics background from $Z\gamma$ events (which essentially cuts off by $\not{E}_T \simeq 40$ GeV) and reduces backgrounds from other sources. The results of our calculation are summarized in Table IV. We see that the physics backgrounds that we have computed are completely negligible.

We expect though that the dominant background could well come from instrumental effects when a jet or lepton is misidentified as a photon. Although a calculation of this detector-dependent background is beyond the scope of the present analysis, we attempt to obtain a rough estimate by computing the inclusive Z background for $\not{E}_T \geq 100$ GeV and then multiplying this by the probability for a jet to fake a photon. We found this inclusive Z background cross section to be 192 fb from $t\bar{t}$ production, 36.7 fb from Zj production and 10.2 fb from $WZ + ZZ$ production, giving a total of 239 fb. Assuming that the probability for a jet to fake a photon is $\sim 2 \times 10^{-4}$ [25], and further that there are typically ~ 5 (10) jets with $E_T \geq 25$ GeV in these LHC events, we obtain the "fake $\gamma + Z$" background cross section of $239 \times 2 \times 10^{-4} \times 5(10) \sim 0.24(0.47)$ fb. We see from Table IV that this reducible background can potentially be comparable to the signal. Furthermore, since this estimate does not include the effects of cracks and other real-world detector effects, it is likely to be increased once these effects are incorporated. We conclude that *unless these reducible backgrounds can be controlled* it is unlikely that the inclusive $Z\gamma$ channel will increase the reach. But with excellent jet-γ rejection, the LHC reach for model line E could be as large as ~ 155 TeV. Moreover, if the signal is truly rate-limited (which does not seem to be the case with our assumptions about the instrumental backgrounds), the reach would grow significantly with the size of the data sample.

IV. SUMMARY AND CONCLUDING REMARKS

The CERN LHC is generally considered as the accelerator facility at which weak scale supersymmetry will either be discovered or definitely excluded. This is because the LHC experiments are expected [11,12,14–16] to probe $m_{\tilde{g}}$ out to 2 TeV, at least within the mSUGRA framework. This extends well beyond the generally accepted bounds from naturalness considerations. Moreover, experiments at the LHC should be able [26] to probe gluinos and squarks beyond 1 TeV even in the experimentally unfavourable scenario where R-parity violating interactions cause the neutralino LSP to decay hadronically, thereby reducing the $\not{E}_T$ as well as degrading the lepton isolation in SUSY events. Although not in themselves a "proof", it is precisely such studies that have led to the general belief that the LHC will be the definitive machine that will test SUSY. In this study, we have added to this evidence by examining the SUSY reach of the LHC within the GMSB framework with SUSY broken at a scale of a few hundred TeV. In this case, the gravitino is then the LSP and SUSY signatures are governed by the nature of the NLSP which then decays into the gravitino and SM particle(s). In our analysis, we conservatively assume that the NLSP decay is prompt, and do not attempt to use the possible presence of a displaced vertex to enhance the SUSY signal.

We divide our study along various model lines introduced in Section I. For each of these

model lines, the NLSP (which is almost always produced as the penultimate product of the sparticle decay cascade) decays via characteristic modes, which can then be used to enhance the SUSY signal, or even to narrow down the model parameters. We do not attempt the latter in the present study. For model line A which was studied in Ref. [5], for instance, $\widetilde{Z}_1 \to \gamma \widetilde{G}$, so that the presence of hard, isolated photons in SUSY events served to distinguish signal from SM backgrounds, resulting in a SUSY reach that corresponding to $m_{\tilde{g}} \leq 2.8$ TeV, to be compared with a reach of about 2 TeV expected within the mSUGRA framework.

In this paper we have examined the LHC reach for four other model lines corresponding to (B) the stau NLSP scenario, (C) the co-NLSP scenario where all three flavours of light charged sleptons are essentially degenerate, and two higgsino-like NLSP scenarios where NLSP decays to (D) the light Higgs boson and (E) the Z boson, dominate. The usual strategy for SUSY searches via $\not{E}_T$ and multilepton events will probe gluino masses up to about 2 TeV, except in the co-NLSP model line where the fact that selectrons and smuons are produced in many cascade decay chains leads to a plethora of $\not{E}_T$ events with ≥ 4 isolated leptons (e or μ) which have very small SM backgrounds. In this case the reach of the LHC extends to $m_{\tilde{g}} = 3$ TeV! For model lines B and D, however, we found that whereas the decays of the NLSP may result in events that are characteristic of the particular model line, signals with identified τ leptons or tagged b jets do not, in general, extend the SUSY reach beyond what is obtained via standard multilepton analyses. For model line E, some enhancement of the reach might be possible via the inclusive $Z\gamma$ channel which is rate-limited, but only if superb jet-γ discrimination is possible. Nevertheless, it should be kept in mind that it will be worthwhile to search for these characteristic events in any LHC data sample enriched in SUSY events, as they will point to the underlying theory, and possibly also lead to a measurement of some of the model parameters [7].

TABLE I. The $\Lambda = 120$ TeV and $\Lambda = 160$ TeV signal cross section in fb for multiple τ-jets plus lepton plus $\not{E}_T$ events for model line B.

	$\Lambda = 120$ TeV				$\Lambda = 160$ TeV			
	0τ	1τ	2τ	$\geq 3\tau$	0τ	1τ	2τ	$\geq 3\tau$
0ℓ	1.75	1.55	0.62	0.02	0.16	0.21	0.09	0.01
1ℓ	5.55	4.37	1.24	0.16	0.69	0.75	0.26	0.04
$2OS\ell$	2.09	1.47	0.27	0.00	0.30	0.29	0.09	0.02
$2SS\ell$	1.56	1.19	0.39	0.01	0.31	0.23	0.09	0.01
$\geq 3\ell$	4.23	2.08	0.34	0.00	0.75	0.51	0.13	0.01

TABLE II. The signal and $t\bar{t}$ background cross sections in fb and the statistical significance $\frac{N_S}{\sqrt{N_B}}$, assuming an integrated luminosity of 10 fb^{-1}, via the 2 b channel for model line D. We show the results for two choices of mistagging rates as discussed in the text.

$\Lambda(TeV)$	$\sigma_S(2\%)$	$\sigma_B(2\%)$	$\frac{N_S}{\sqrt{N_B}}(2\%)$	$\sigma_S(1\%)$	$\sigma_B(1\%)$	$\frac{N_S}{\sqrt{N_B}}(1\%)$
140	2.11	0.89	7.09	2.05	0.72	7.62
150	1.34	0.89	4.49	1.36	0.72	5.36
160	0.70	0.89	2.34	0.73	0.72	2.72

TABLE III. The SUSY signal cross sections (in fb) for inclusive Z plus $\not{E}_T \geq 230$ GeV events for model line E together with SM backgrounds from Zj, $WZ + ZZ$ and $t\bar{t}$ production. For the case of the $t\bar{t}$ background, the 'Z' is a fake from two leptons accidently reconstructing the Z mass. The signal cross sections are shown in the first three columns for $\Lambda = 140, 150$ and 160 TeV along with the statistical significance for an integrated luminosity of 10 fb^{-1}.

	$\Lambda(140)$	$\Lambda(150)$	$\Lambda(160)$	Zj	$WZ + ZZ$	$t\bar{t}$
$\sigma(fb)$	2.73	2.50	2.22	2.45	0.84	4.13
$N_S/\sqrt{N_B}$	3.17	2.90	2.58			

TABLE IV. The SUSY signal cross sections (in fb) for the inclusive $Z\gamma$ channel for model line E together with physics SM backgrounds from Zj, $WZ + ZZ$, $t\bar{t}$ and $Z\gamma$ production. Here an $\ell^+\ell^-$ pair with a mass within 10 GeV of M_Z is identified as a Z. The signal cross sections are shown for $\Lambda = 140, 150$ and 160 TeV. See also the discussion in the text about potential instrumental backgrounds to this signal.

	$\Lambda(140)$	$\Lambda(150)$	$\Lambda(160)$	Zj	$WZ + ZZ$	$t\bar{t}$	$Z\gamma$
$\sigma(fb)$	0.78	0.59	0.40	0.0048	0.0031	0	1.5×10^{-4}

REFERENCES

[1] V. Ruhlmann-Kleider, *Plenary talk presented at the 1999 Lepton-Photon Symposium*, SLAC, Stanford, hep-ex/0001061 (2000); A. Savoy-Navarro, in *Proc. Euro. Phys. Society Meeting*, Tampere, Finland, July (1999), Fermilab-Conf-99/281-E (1999).

[2] H. Baer, M. Díaz, P. Quintana and X. Tata, hep-ph/0002245 (2000).

[3] M. Dine and A. Nelson, Phys. Rev. **D48**, 1277 (1993); M. Dine, A. Nelson, Y. Shirman, Phys. Rev. **D51**, 1362 (1995); M. Dine, A. Nelson, Y. Nir and Y. Shirman, Phys. Rev. **D53**, 2658 (1996).

[4] S. Dimopoulos, M. Dine, S. Raby and S. Thomas, Phys. Rev. Lett. **76**, 3494 (1996); S. Dimopoulos, S. Thomas and J. Wells, Phys. Rev. **D54**, 3283 (1996) and Nucl. Phys. **B488**, 39 (1997); S. Ambrosanio *et al.*, Phys. Rev. Lett. **76**, 3498 (1996) and Phys. Rev. **D54**, 5395 (1996); K. S. Babu, C. Kolda and F. Wilczek, Phys. Rev. Lett. **77**, 3070 (1996); H. Baer, M. Brhlik, C. H. Chen and X. Tata, Phys. Rev. **D55**, 4463 (1997); J. Bagger, K. Matchev and D. Pierce, Phys. Rev. **D55**, 3188 (1997); R. Rattazzi and U. Sarid, Nucl. Phys. **B501**, 297 (1997); D. Dicus, B. Dutta and S. Nandi, Phys. Rev. Lett. **78**, 3055 (1997) and Phys. Rev. **D56**, 5748 (1997); K. Cheung, D. Dicus, B. Dutta and S. Nandi,Phys. Rev. **D58**, 015008 (1998); B. Dutta, D. J. Mueller and S. Nandi, Nucl. Phys **B 544**, 451 (1999) ; D. J. Mueller and S. Nandi, Phys. Rev. **D60**, 015008 (1999); S. Martin and J. Wells, Phys. Rev. **D59**, 035008 (1999); S. Ambrosanio and Eur. J. Phys. **C12**, 287 (2000); See G. Giudice and R. Rattazzi, Phys. Rep. **322**, 419 (1999) for a review.

[5] H. Baer, P.G. Mercadante, X. Tata and Y. Wang, Phys. Lett. **B435**, 109 (1998).

[6] H. Baer, P.G. Mercadante, X. Tata and Y. Wang, Phys. Rev. **D60**, 55001 (1999).

[7] F. Paige and I. Hincliffe, Phys.Rev. **D60**, 095002 (1999).

[8] K. Matchev and S. Thomas, hep-ph/9908482 (1999).

[9] B. Abbott *et al.* Phys. Rev. Lett. **80**, 442 (1998); F. Abe *et al.* Phys. Rev. Lett. **81**, 1791 (1998) and Phys. Rev. **D59**, 092002 (1999).

[10] R. Barate *et al.* Phys. Lett. **B429**, 201 (1998) and CERN-EP/99-171 (1999); M. Acciarri *et al.* Phys. Lett. **B470**, 268 (1999).

[11] H. Baer, C. Chen, F. Paige and X. Tata, Phys. Rev. **D52**, 2746 (1995).

[12] H. Baer, C. Chen, F. Paige and X. Tata, Phys. Rev. **D53**, 6241 (1996).

[13] H. Baer, F. Paige, S. Protopopescu and X. Tata, hep-ph/9810440 (1998).

[14] ATLAS Technical Proposal, CERN/LHCC/94-43 (1994) .

[15] CMS Technical Proposal, CERN/LHCC 94-38 (1994).

[16] S. Abdullin *et al.* CMS NOTE 1998/006, hep-ph/9806366.

[17] H. Lai *et al.*, (CTEQ Collaboration), Phys. Rev. D**51**, 4763 (1995).

[18] V. Barger, A. Stange and R.J.N. Phillips, Phys. Rev. **D44**, 1987 (1991).

[19] V. Barger, T. Han and H. Pi, Phys. Rev. **D41**, 824 (1990).

[20] V. Barger and T. Han Phys. Lett. **B212**, 117 (1988).

[21] H. Baer, C. Chen, F. Paige and X. Tata, Phys. Rev. **D49**, 3283 (1994).

[22] H. Baer, M. Bisset, X. Tata and J. Woodside, Phys. Rev. **D46**, 303 (1992).

[23] I. Hinchliffe, F. Paige, M. Shapiro, J. Soderqvist and W. Yao, Phys. Rev. **D55**, 5520 (1997).

[24] H. Baer, X. Tata and J. Woodside, Phys. Rev. **D42**, 1450 (1990).

[25] F. Gianotti, private communication.

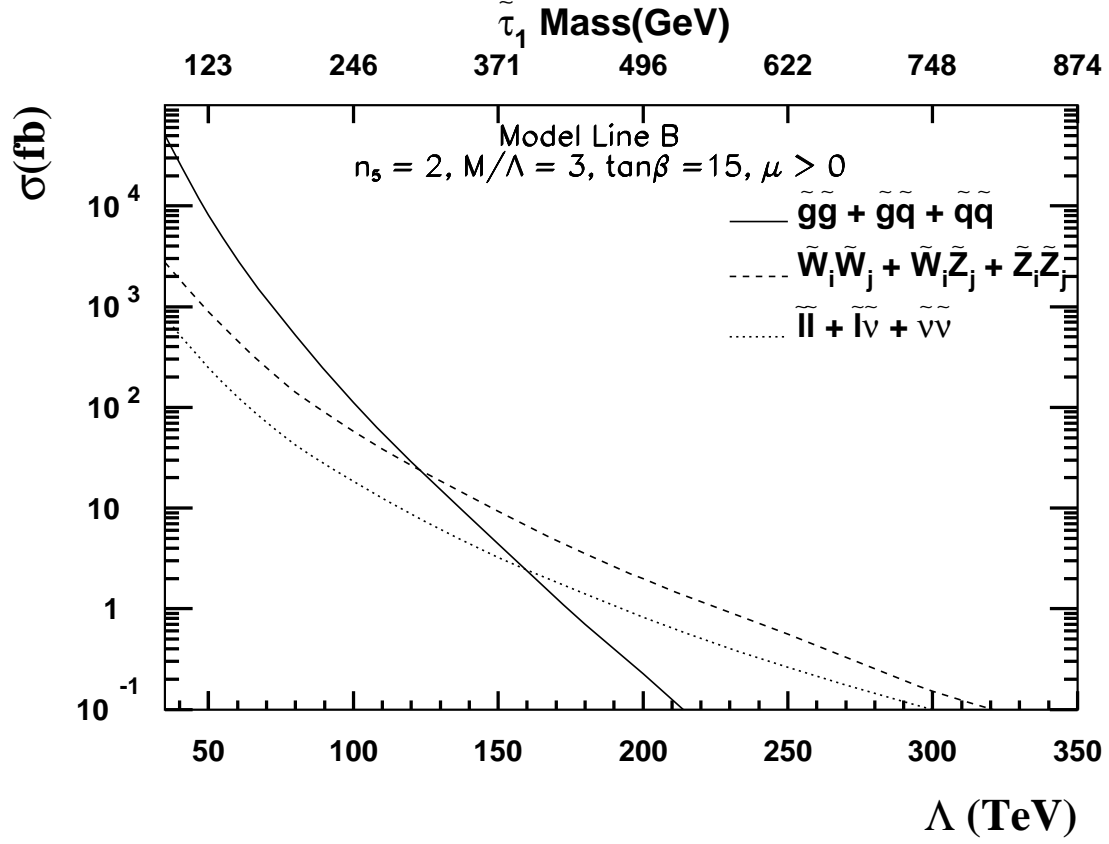[26] H. Baer, C. Chen and X. Tata, Phys. Rev. **D55**, 1466 (1997).

FIG. 1. Sparticle production cross sections versus Λ for various sets of SUSY processes at a 14 TeV pp collider within the GMSB framework for the $\tilde{\tau}_1$ NLSP model line B. For sleptons, we sum over the first two families.
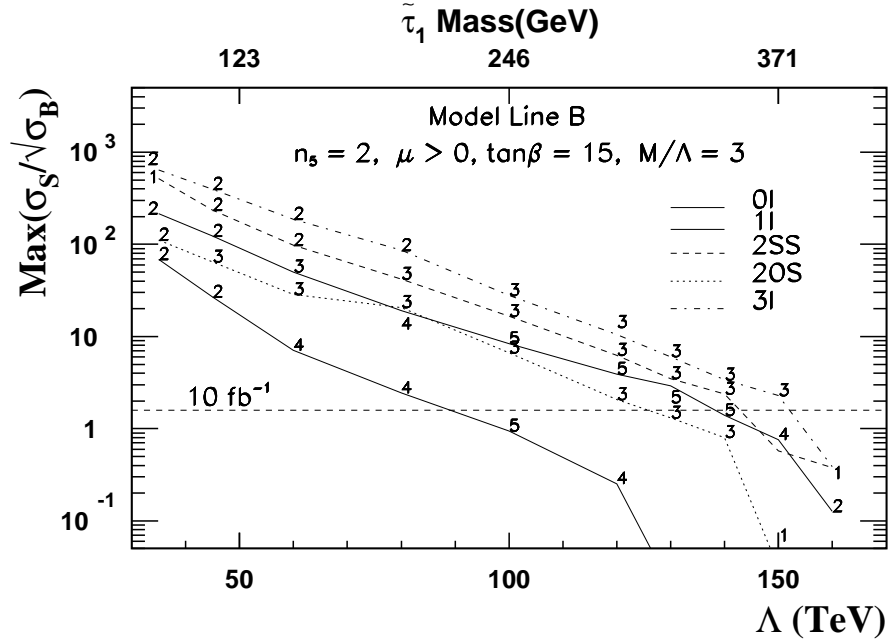
FIG. 2. We show the max $\sigma_S/\sqrt{\sigma_B}$ with respect to E_T^c versus Λ for model line B for $0\ell+ \not{E}_T$ and the various multilepton channels introduced in the text. We evaluate $\sigma_S/\sqrt{\sigma_B}$ for $E_T^c = 100, 200, 300, 400$ and 500 GeV and choose the value of E_T^c that maximizes this, subject to a minimum signal cross section of 0.5 fb. For each value of Λ for which we evaluate the signal, the number denotes this optimal choice of E_T^c, $e.g$ 2 denotes $E_T^c = 200$ GeV, etc. The horizontal line shows the minimum cross section for a 5σ signal, assuming an integrated luminosity of 10 fb^{-1}.
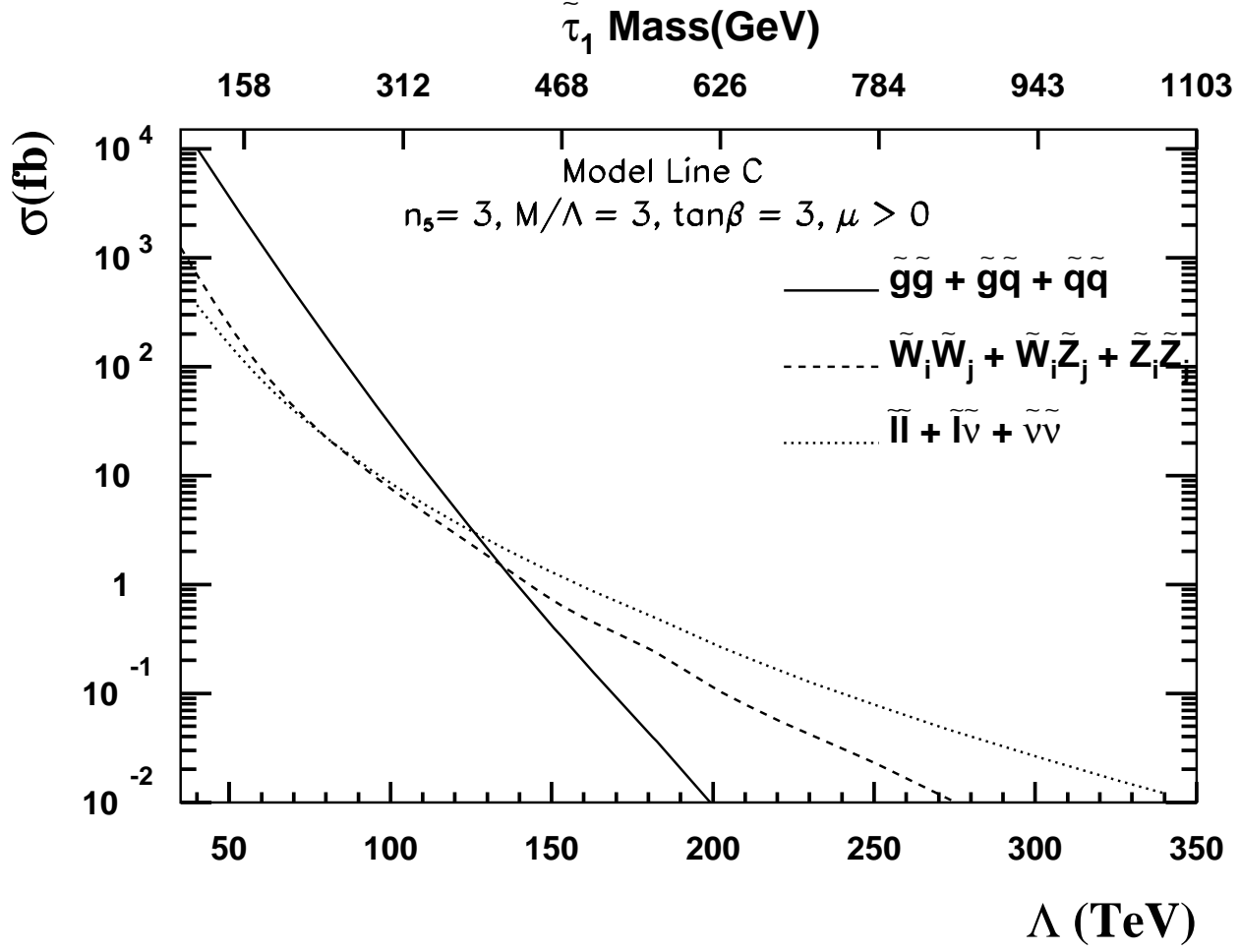
FIG. 3.   The same as Fig. 1 except that the cross sections are now shown for model line C.
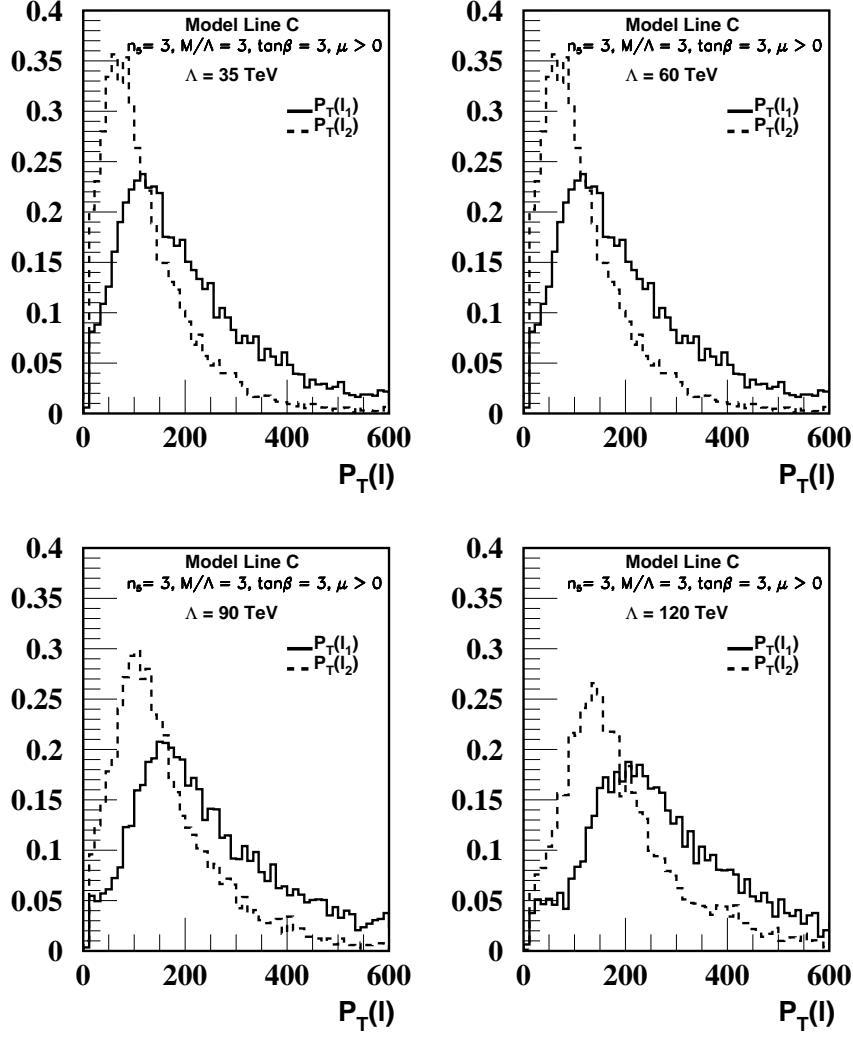
FIG. 4. The transverse momentum distributions for the hardest (solid) and second hardest (dashed) leptons for four choices of Λ for model line C.
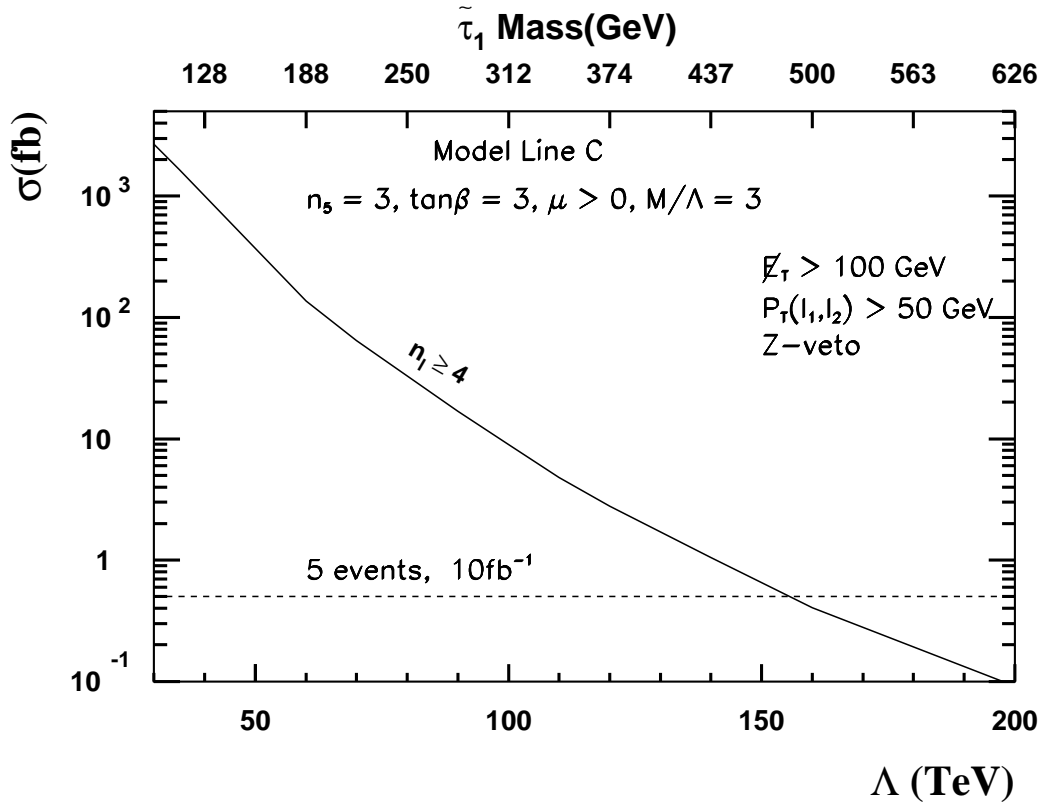
FIG. 5. The SUSY signal cross section for the inclusive $n_l \geq 4$ channel for model line C after all the cuts discussed in the text. The SM background in this channel is negligible. The horizontal line denotes the cross section corresponding to the 5 event level for an integrated luminosity of $10 \ fb^{-1}$.
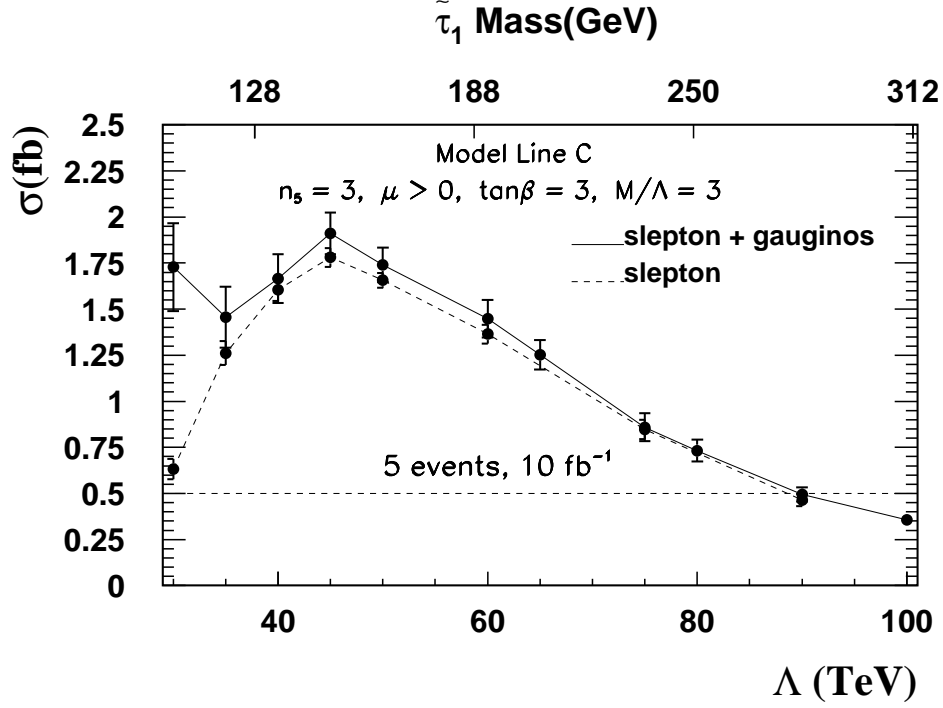
FIG. 6. The signal cross section from slepton pair production (dashed) and slepton, chargino and neutralino production (solid) in the opposite sign dilepton channel after cuts designed to optimize the slepton signal for model line C. The dots correspond to the values of Λ for which we did the simulation. The horizontal line denotes the minimum observable level for a 5σ signal at the LHC assuming an integrated luminosity of 10 fb^{-1}. The reach of $\Lambda = 90$ TeV corresponds to $m(\tilde{\ell}_R) = 280$ GeV.
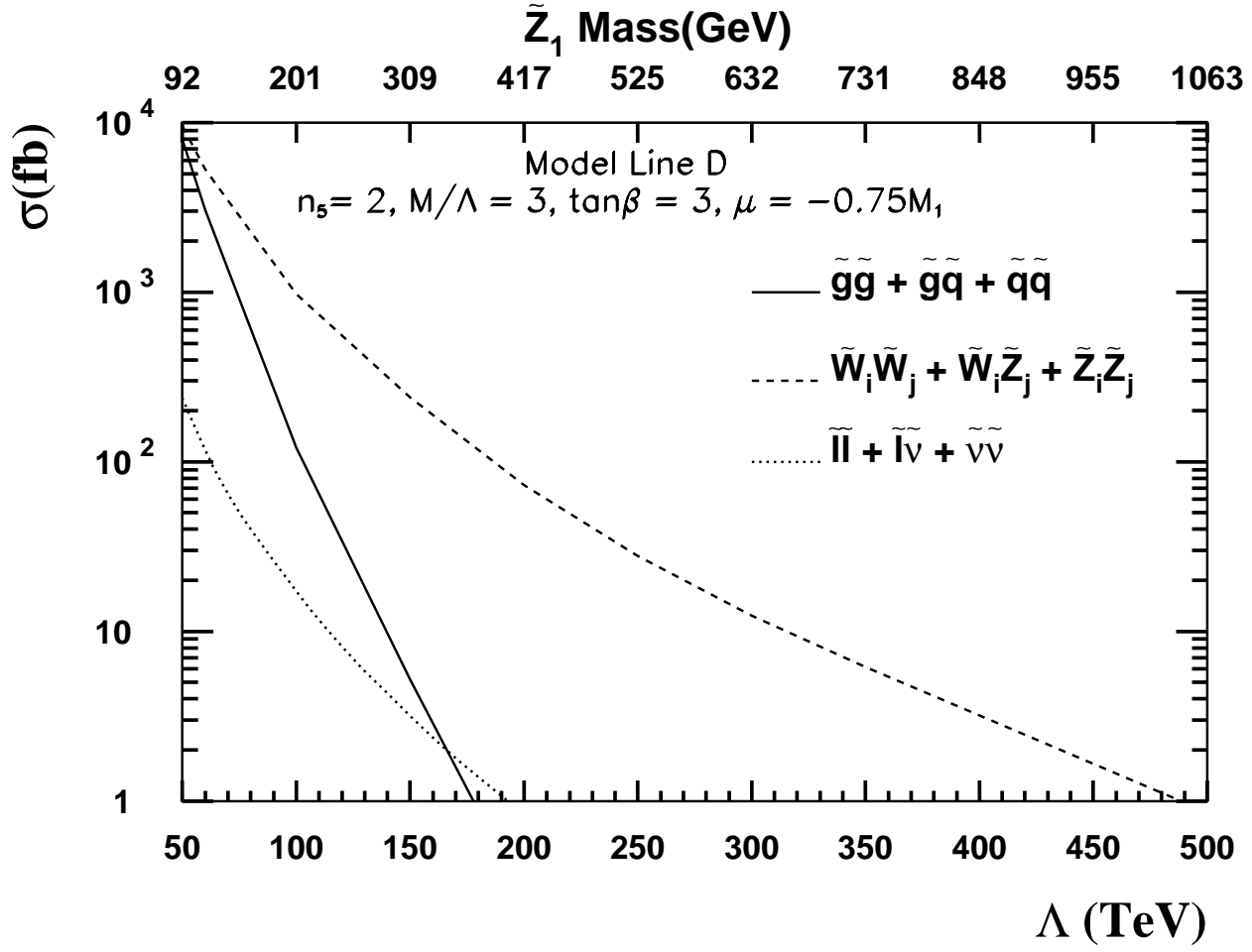
FIG. 7.   The same as Fig. 1 except that the cross sections are now shown for model line D.
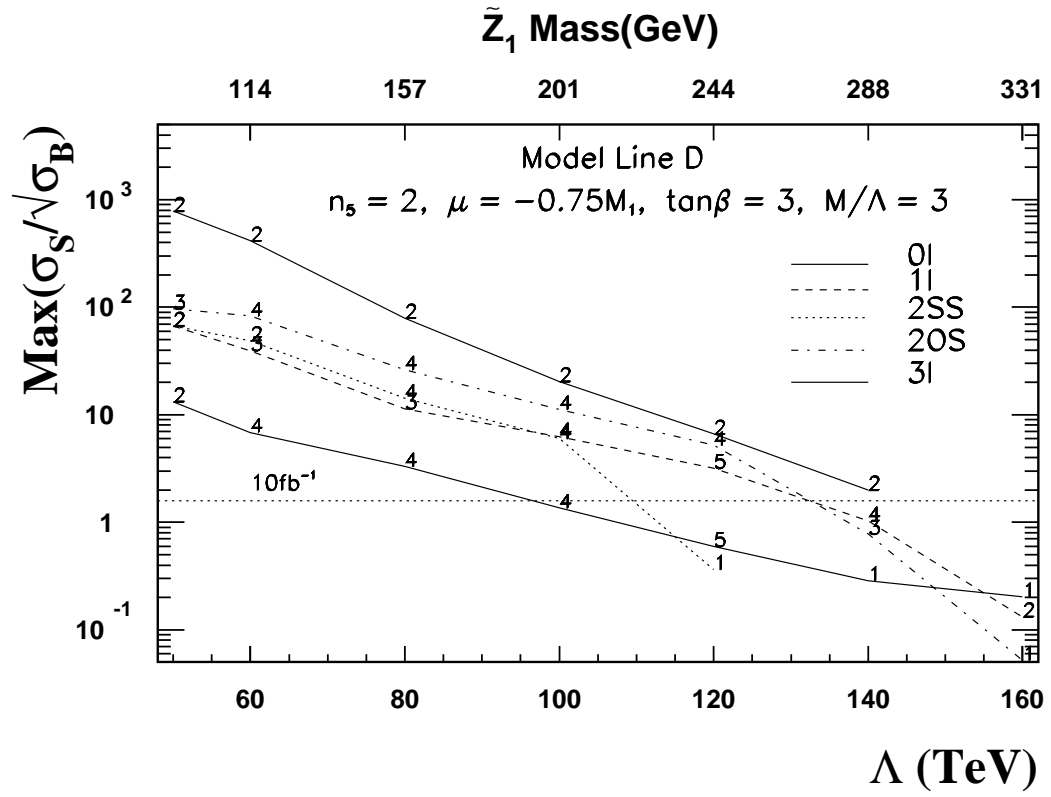
FIG. 8. The same as Fig. 2, but for the higgsino NLSP model line D. Notice though that the legends for the various channels are different.
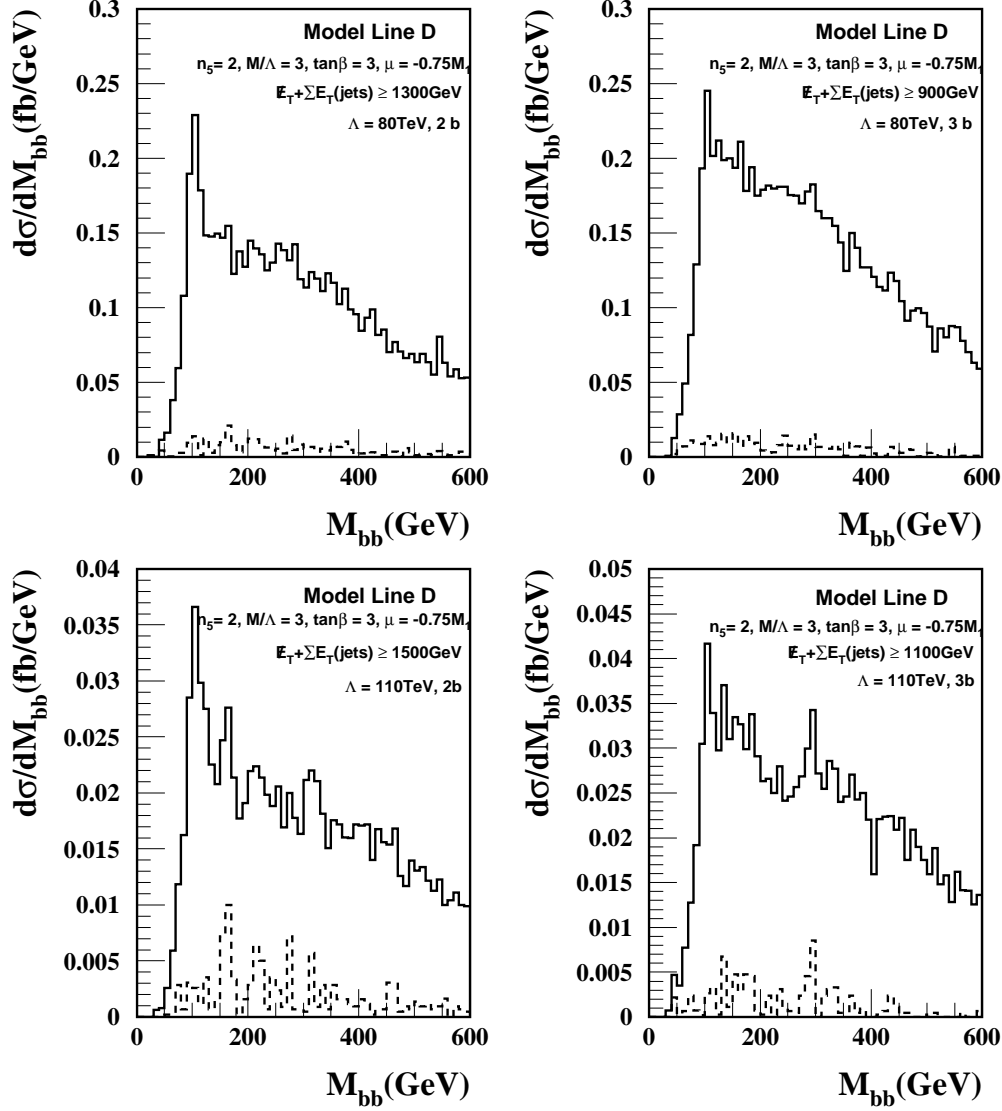
FIG. 9. The M_{bb} distribution for events after all cuts discussed in the text in the two tagged b and 3 tagged b channels for the higgsino model line D. We illustrate the results for $\Lambda = 80$ and 110 TeV. The solid histogram is the signal plus background, while the dashed line is just the $t\bar{t}$ background.
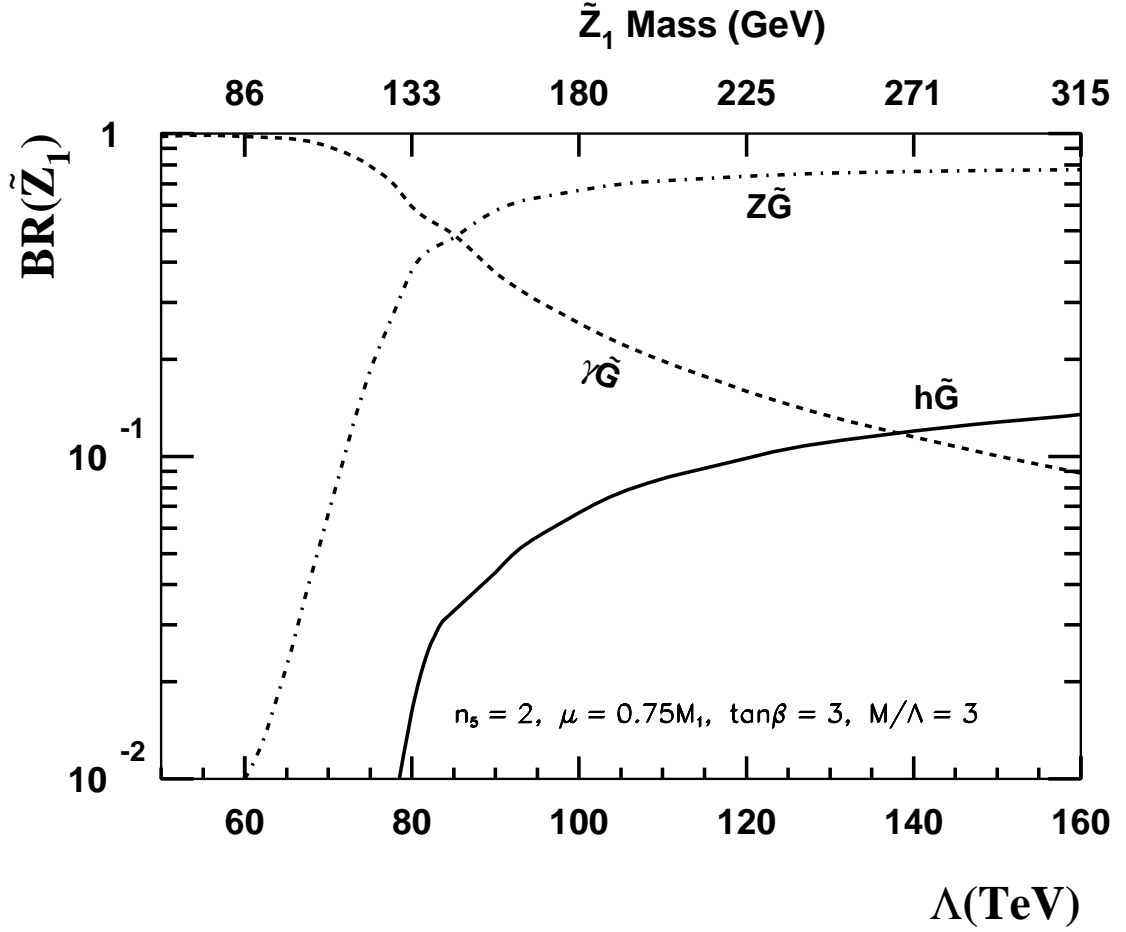
FIG. 10. The branching fractions for various decays of the neutralino NLSP in model line E versus the parameter Λ. The scale on top shows the NLSP mass.
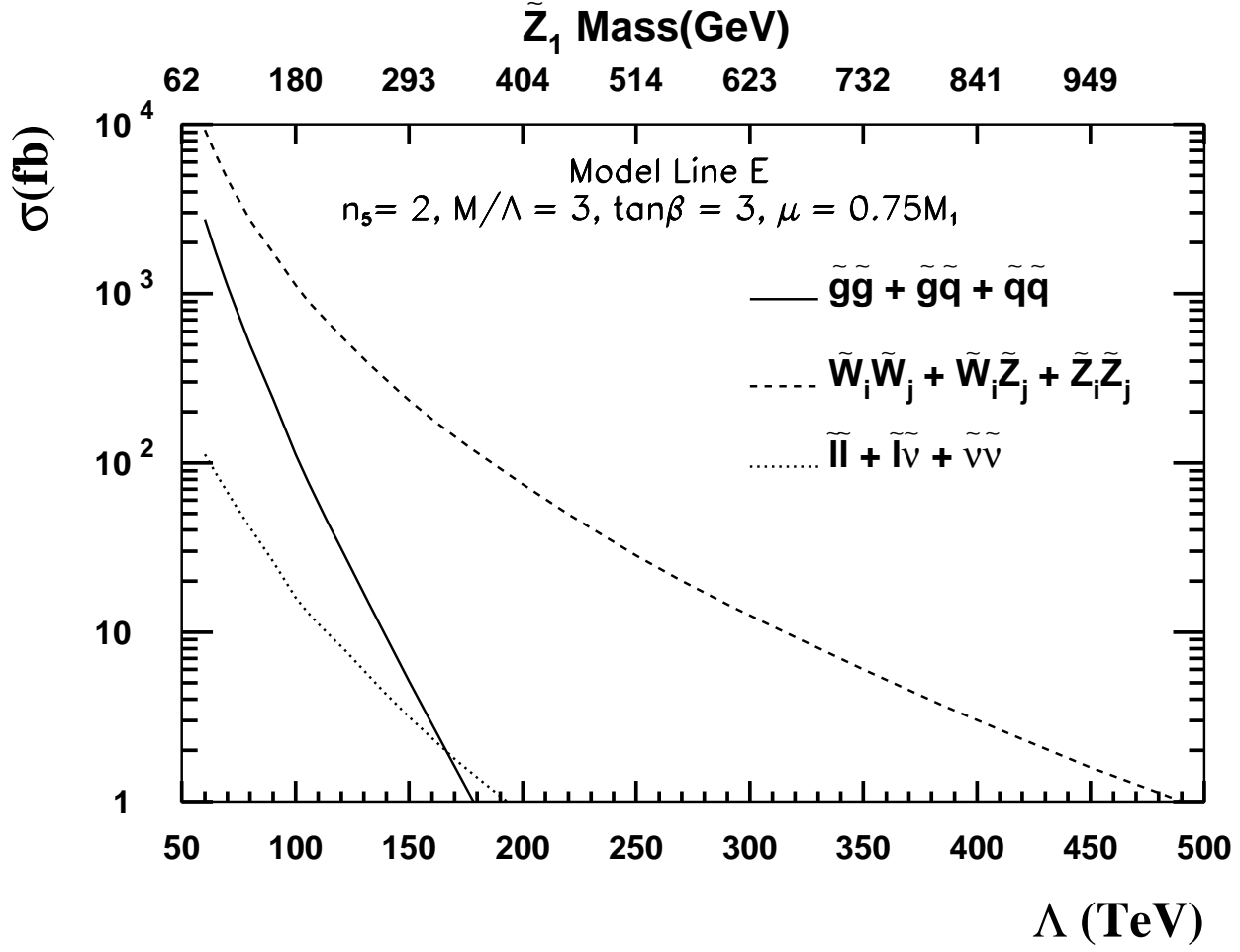
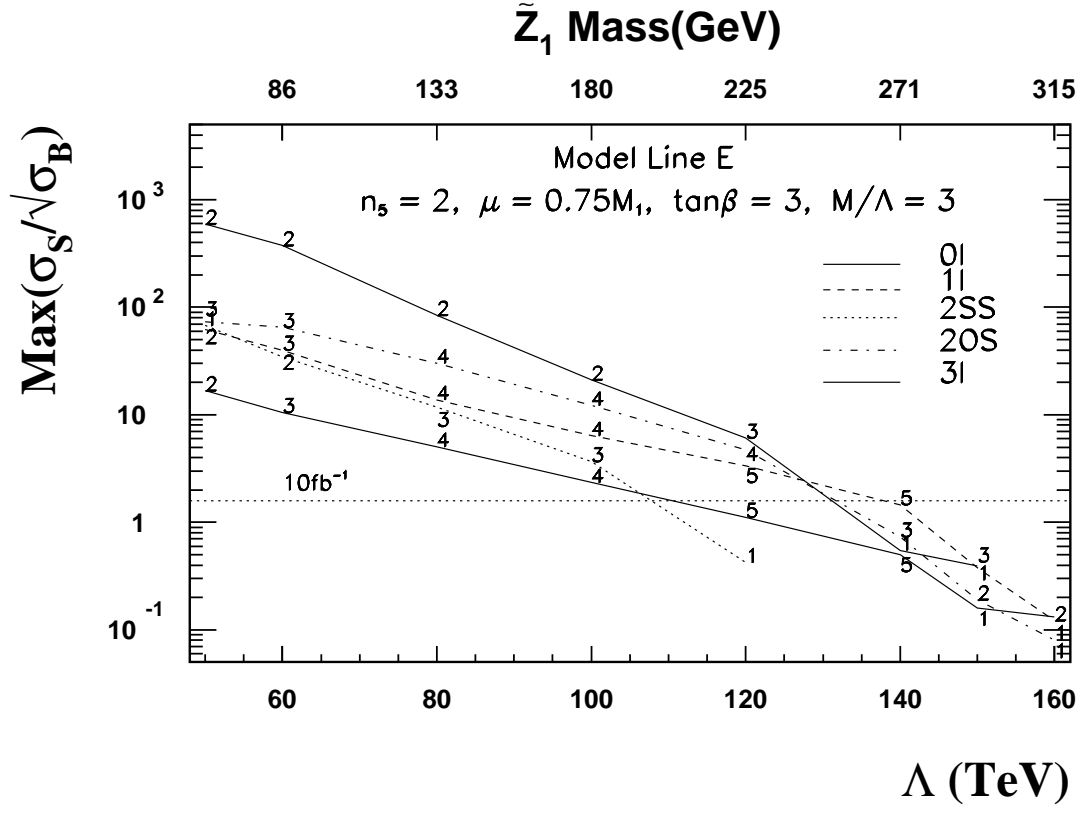FIG. 11. The same as Fig. 1 except that the cross sections are now shown for model line E.

FIG. 12. The same as Fig. 8, but for the higgsino model line E.